Temperatures in flowing cascaded arc : model vs experiments

TEMPERATURES IN A FLOWING CASCADED ARC: MODEL VS EXPERIMENTS

J.J. Beulens, G.M.W. Kroesen, H. de Regt, P.M. Vallinga and D.C. Schram,
University of Technology, Dept. of Physics,
P.O.Box 513, 5600 MB Eindhoven.

ABSTRACT

The cascaded arc described here is used as a particle source for fast a–C:H deposition. The arc burning on argon at high flows (about 100 scc/s) is investigated numerically and experimentally. Numerically the pressure, temperatures and electron density in the arc are calculated as a function of the axial position with a one dimensional model using conservation laws for mass, energy and momentum. Experimentally these parameters are measured using optical diagnostics.

INTRODUCTION

Since about 1985 a cascaded arc is used as a particle source in the deposition machine described by Kroesen[1]. This method of deposition showed to be very fast and efficient to grow amorphous carbon films (a–C:H), varying from graphite and diamond to polymers[1,2]. The most important difference of this method, with respect to R.F. techniques, is that the three most important functions of a deposition process, as there are dissociation and ionization, transport and deposition, are spatially separated. The dissociation takes place in a cascaded arc burning on argon. The temperatures in the arc are about 10000–12000 K. At the end of this arc hydrocarbons are injected which are then dissociated and ionized effectively. At the end of the arc the plasma expands supersonically into a vacuum vessel. That means that the plasma cools down and the formed hydrocarbon fractions are transported towards the substrate, where an amorphous carbon film can grow. The quality of the films depend mainly on the amount of energy available for each injected carbon atom. The behavior of the refractive index as a function of this energy could be a confirmation that in our deposition method the carbon ions rather than radicals govern the deposition process[1,3,4]. Therefore the cascaded arc is investigated numerically and experimentally in order to improve the ionization efficiency. The conservation laws for mass, momentum and energy for both the electrons and the heavy particles are solved by Runge–kutta integration methods. The obtained results are then compared to the experimental data, obtained by optical diagnostics.

EXPERIMENTAL SET UP

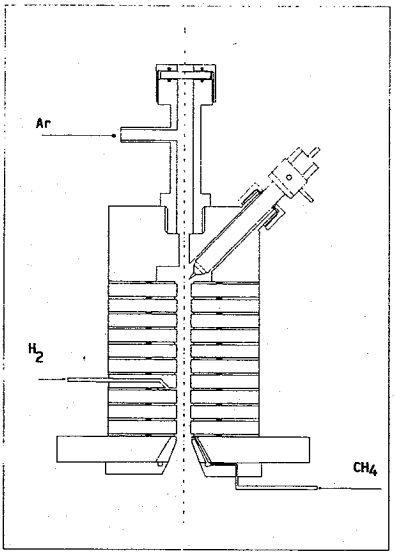

Fig. 1 Outline of the cascaded arc as a particle source.

The cascaded arc (fig.1) used in this work, consists of a stack of ten water cooled copper plates insulated electrically from each other by plastic spacers and O–rings, three tungsten–thorium cathodes on one end and an anode on the other. Through the copper plates and the anode plate there is a bore of 4 mm, forming a cylindrical channel of 6 cm. The argon gas is fed through mass flow controllers and then injected at the cathode side. The gas or plasma is extracted through a nozzle in the anode plate which is mounted on a vacuum vessel. The pressure in the vessel is about 1 mbar, whereas the pressure in the arc is about 0.5 bar. This means that the plasma will be extracted supersonically. For the experiments the cascaded arc has two special features to measure the plasma pressure and to couple out the emitted light. The pressure is measured by a MKS baratron pressure transducer. The light is coupled out through an optical fiber and coupled in an optical system (fig. 2). Between the two

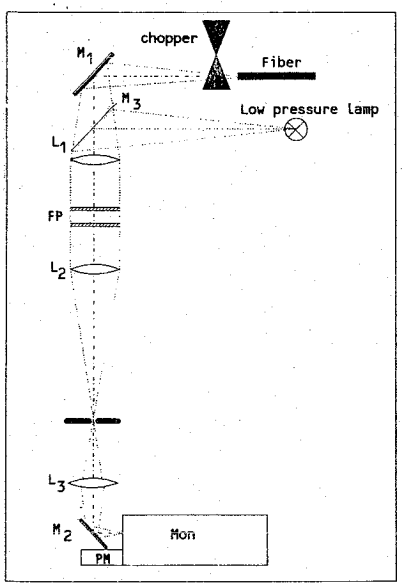

Fig. 2 Optical system, consisting of several mirrors (M 1,2 and 3), a chopper, a diaphragm, several lenses and a Fabry–Perot interferometer. The fiber directs the light of the arc into the optical system.

lenses L1 and L2 the light beam is parallel and thus a fabry perot interferometer can be placed here. The light source in figure 2 is a hollow cathode arc or a glow discharge on argon, to make a wavelength reference and to measure the apparatus profile. Lens L2 images the exit of the fiber on diaphragm D1. Finally, lens L3 images the diaphragm on the entrance slit of the monochromator (Jarrell–Ash 0.5 m). On the exit slit a photo multiplier is mounted. In case the interferometer was not used 10 μm slits were used, otherwise 100 μm slits were placed in the monochromator.

PLASMA DIAGNOSTICS

The wavelength dependent intensity profile of a spectral line emitted by the plasma is determined by several physical effects. Each effect can result in a shift of the line position and or in a broadening of the line profile with either a gauss or a lorentz like contribution:

$$I_g(\omega) = \frac{1}{\Delta\omega_d\sqrt{\pi}} \exp\left[-\left(\frac{\omega-\omega_0}{\Delta\omega_d}\right)^2\right] \qquad (1)$$

$$I_l(\omega) = \frac{\gamma}{2\pi} \frac{1}{(\omega-\omega_0)^2+(\gamma/2)^2} \qquad (2)$$

where ω is the angular frequency, ω_0 the central resonance frequency, $\Delta\omega_d$ the width at $1/e^2$ of the top of intensity I_g and γ is the full width at $1/2\ I_l$. When more broadening mechanisms occur the line shape is in many cases a Voigt profile, which is a convolution of a Gaussian and a Lorentzian profile.

Doppler broadening gives rise to a gauss profile with width $\Delta\omega_d=(\omega/c)\sqrt{(2kT_h/m)}$ (at $1/e^2$), where k is the Boltzmann constant, m is the mass of the emitting particle, c is the speed of light and T_h is the heavy particle temperature. Also a shift of the central line occurs when there is a net velocity of the particles which makes an angle with the line of sight other than 90^0: $\Delta\lambda=-\lambda_0\cos\theta/c$, where $\Delta\lambda$ denotes the wavelength shift and λ_0 is the central undisturbed wavelength.

Another important broadening mechanism is Stark broadening. The quadratic Stark effect, which is the influence of charged particles on the energy levels of the emitting atom, give a Lorentz profile[5,6]. This stark effect gives for the (FWHM)width and shift respectively:

$$\gamma = Nv^{1/3}C_4^{2/3}\,(\pi/2)^{2/3}\,\pi \qquad (3)$$

$$\Delta = -\gamma/1.15 \qquad (4)$$

where N is the density of the disturbing particle and C_4 a constant which value is about 10^{-22} m^4s^{-1} for neutral argon atoms. For hydrogen the profiles are not Lorentz like[5,6]. The (FWHM) width gives the electron density: $n_e = C(\Delta\lambda)^{3\ 2}$
in which C is a constant in the order of 1.2 10^{22} m^{-3} $nm^{3\ 2}$ (for Hβ and T= 1 eV).

The line to continuum ratio provides the electron temperature using the equation:

$$T_e = \frac{E_p}{k} \ln^{-1}\left[\frac{I_{lijn}}{I_{cont}}\right]_{top} \frac{A_{pq}hc\lambda\, g_p\sqrt{T_e}}{4\pi\omega_i C_l \Delta l n_e} \qquad (5)$$

where ω_i is the partition function of the ArII system[7], g_p the statistic weight of the upper level and E_p the energy difference between the upper level p and the ion ground state, C_l=1.63 10^{-43} $Wm^4K^{1\ 2}sr^{-1}$ a constant, n_e the electron density and A_{pq} the transition probability from level p to q for spontaneous emission.

With the summed broadening effects we are able to measure both the heavy particle temperature and the electron temperature and also the electron density, when the line profiles are measured using a Fabry Perot interferometer and deconvoluted into Gauss and Lorentz parts. With the described optical system we simply can do this by inserting the fiber or directly in front of the entrance slit of the monochromator or in the focal point of lens L_1(see fig. 2). In the latter case the F.P. can be used or left out.

MODEL

Recently de Haas has investigated the physics of a strongly flowing, fully equilibrated cascaded arc plasma [8]. The evolution of the electron density as a function of the axial position in the arc channel however indicates that the plasma is not in local thermal equilibrium (LTE), especially in the beginning of the channel. Kroesen [1] has developed a model which allows ionization and thermal non–equilibrium. With this model, which does not include the effects of viscosity, the evolution of the electron density and the heavy particle temperature can be obtained as a function of the axial position in an argon arc.

In the present work, this model has been extended in order to describe the evolution of the plasma properties as a function of the axial position in the arc self consistently. This implies that, besides the evolution of the electron density and the heavy particle temperature, the evolution of the plasma velocity, discharge pressure, and the electron temperature have been included. The physical phenomena that are taken into account are: direct or indirect ionization by electron impact, three particle recombination, radiative recombination and energy exchange between different species due to elastic collisions.

In the present model also the wall friction has been included. It has been shown [9] that for sufficiently large electron densities almost every excitation of an atom in an arc plasma eventually leads to ionization. Therefore, excitation will be treated as ionization.

In order to describe the evolution of particle densities, flow velocity and temperatures, we use the conservation laws for mass, momentum and energy. The argon atoms, density n_h, and the argon ions, density n_h^+, will be treated together as far as their transport properties are concerned. Hence, we assume that the drift velocities of the heavy particles are approximately equal, i.e. $\underline{w}_h \simeq \underline{w}_h^+ \simeq \underline{u}$. The electron number balance can now be written as

$$\nabla\cdot(n_e\underline{u}) = n_e(n_h - n_{hs})K_i - n_e n_h^+(K_r\Lambda) \equiv S_e\,, \tag{6}$$

where K_i represents the combined rate coefficient for excitation and ionization, $K_r\Lambda$ is the rate coefficient for radiative recombination corrected for local absorption, and n_{hs} is the density of hydrogen atoms according to the Saha equation. Three particle recombination is taken into account in equation (6) by applying the method of detailed balancing [10]:

$$n_e^2\, n_h^+\, K_{r3} = n_e\, n_{hs}\, K_i\,, \tag{7}$$

where K_{r3} is the rate coefficient for three particle recombination.

The number balances for the argon atoms read

$$\nabla\cdot(n_h\underline{u}) = -\,n_e(n_h - n_{hs})K_i + n_e n_h^+(K_r\Lambda) \equiv S_h\,. \tag{8}$$

If the momentum balances of all species present in the plasma are added, the result is:

$$\rho(\underline{u}\cdot\nabla)\underline{u} + \nabla p + \nabla\cdot\Pi = 0\,, \tag{9}$$

where Π is the viscosity tensor, and the mass density ρ is defined as $\rho = m_h(n_h + n_h^+)$. Assuming that the heavy particles all have the same temperature T_h, the total energy balance for all heavy particles reads

$$\nabla\cdot(\tfrac{3}{2}n_t k T_h\underline{u}) + n_t k T_h(\nabla\cdot\underline{u}) = -\nabla\cdot\underline{q}_h - \Pi_o{:}\nabla\underline{u} + Q_{eh} \equiv Q_h\,, \tag{10}$$

where $\underline{q}_h$ denotes the heavy particle heat flux ($\underline{q} = -\kappa\nabla T$), Π_o the viscosity tensor and Q_{eh} the elastic energy transfer between electrons and heavy particles:

$$Q_{eh} = 3n_e k(T_e - T_h)\left[\frac{m_e}{m_h}\,(\nu_{ei}^h + \nu_{eo}^h)\right]. \tag{11}$$

where, ν_{ei}^h and ν_{eo}^h denote the collision frequencies of an electron with argon ions and atoms respectively. To complete the set of equations the electron energy balance is needed:

$$\nabla\cdot(\tfrac{3}{2}n_e k T_e\underline{u}) + n_e k T_e(\nabla\cdot\underline{u}) = -\nabla\cdot\underline{q}_e - \Pi_e{:}\nabla\underline{u} - n_e(n_h - n_{hs})K_1 E_{ion} + \tag{12}$$
$$- n_e^2(K_r\Lambda)\tfrac{3}{2}k T_e - 4\pi C_1 n_e^2 \langle Z\rangle T_e^{\frac{1}{2}}\,\frac{k}{hc}\,\xi_{ff} - Q_{eh} - Q_{line} - Q_{rec} + Q_{ohm} \equiv Q_e\,.$$

The term containing ξ_{ff} represents the inelastic free–free transitions (Brehmsstrahlung), whereas Q_{line} and Q_{rec} denote the energy losses of the electrons caused by escape of line radiation and by escape of radiation resulting from recombination to excited levels. The Ohmic heating is denoted by $Q_{ohm} = \underline{j}\cdot\underline{E} = j^2/\sigma$. The electrical conductivity σ of the plasma in the arc channel is evaluated according to the Frost mixture rule [10].

The wall friction factor is given by f, and D is the diameter of the arc channel. Separate measurements [1] in an argon cascaded arc have shown that the relation between the friction factor f and the Reynolds number has a strong resemblance to the

theoretical curve for laminar flow through a perfectly smooth duct. A quasi one–dimensional approach is followed, as is usual in treating nozzle expansions [11]. This implies that the energy and momentum transfer of the plasma to the arc wall are neglected, the radial diffusion and heat conduction terms are neglected because they are much smaller than the axial expansion terms, and that the parameters in the equations are regarded as constant over the arc channel cross section.

We can now obtain a set of differential equations in the variables α, ρ, u, T_e, and T_h. With the definitions $n_e = \alpha\rho/m_h$, $n_h = \rho(1-\alpha)/m_h$, where $\alpha = n_e/(n_e+n_h+n_h^+)$ is the ionization degree, the equations can be written as:

$$\frac{\partial \alpha}{\partial x} = \frac{m_h}{\phi_o} S_e \,, \tag{13}$$

$$\frac{\partial u}{\partial x} = -\frac{Q_t}{E_s} \frac{2m_h u}{\phi_o} \,, \tag{14}$$

$$\frac{\partial T_e}{\partial x} = \frac{Q_t}{E_s} \frac{4m_h T_e}{3\phi_o} + \frac{m_h}{3k\phi_o} \frac{2Q_e - 3kT_e S_e}{\alpha} \,, \tag{15}$$

$$\frac{\partial T_h}{\partial x} = \frac{Q_t}{E_s} \frac{4m_h T_h}{3\phi_o} + \frac{2m_h}{3k\phi_o} Q_e \,, \tag{16}$$

where $Q_t = Q_e + Q_h + 3\rho u^3/4D$, $T_a = T_h + \alpha T_e$ is the effective temperature, and E_s is defined by $E_s = 3m_h u^2 - 5kT_a = 3m_h u^2(1-1/M^2)$, where $M = u/c_{pl}$ is the Mach number, $\phi_o = \rho u = m_h \varphi/A$, and φ is the argon flow. The two–temperature speed of sound c_{pl} can be deduced from (13) to (16): $c_{pl} = \sqrt{(5kT_a/3m_h)}$.

At the end of the arc channel the plasma is accelerated to sonic conditions. In fact, the sonic condition, i.e. $u = c_{pl}$ at the end of the arc channel, must be treated as a boundary condition for the system of equations.

RESULTS

Equations (13) – (16) have been solved for an arc with constant diameter by Runge–Kutta integration using MicroSoft Pascal on an IBM PC/RT. The plasma is flowing through the arc channel at a relatively large velocity. This flow is associated with a pressure drop. Friction with the wall causes the pressure to drop faster than would be expected for an accelerating duct flow without wall interaction. Figure 3 shows the axial profile of the measured and the calculated plasma pressure. There is a good agreement (5%–10% discrepancy) between calculations and experiment.

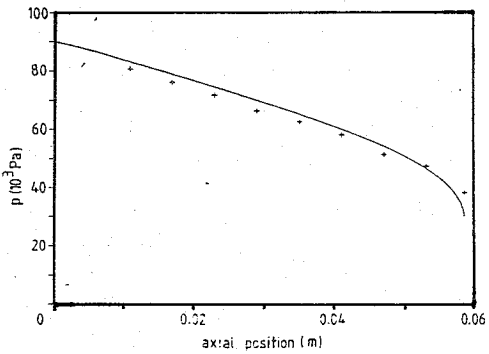

Fig 3: Plasma pressure versus axial position (flow is 200 scc/s, arc current of 50 A, experimental crosses, calculated lines)

Figure 4 shows the axial profile of the experimentally determined electron temperature, as well as the calculated profiles of the electron and gas temperature (heavy particle temperature). As can be seen the electron temperature is nearly constant. The gas temperature is initially lower than the electron temperature. The plasma needs about 30 mm of axial length to relaxate towards temperature equilibrium.

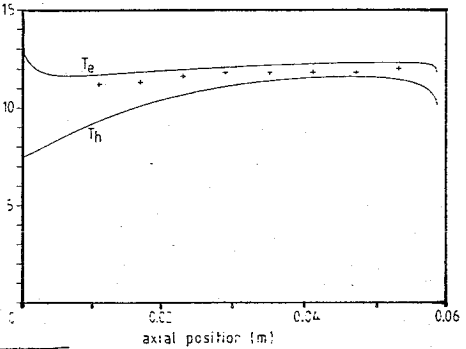

Fig 4: Axial profile of the experimental electron temperature (crosses) and modelled electron and heavy particle temperature (solid lines).

However, a noticeable temperature difference between electrons and heavy particles still remains. At the end of the channel the temperature decreases because of acceleration of the plasma. As can be seen from figure 4, the calculated electron temperature is about 5% too high.

In figure 5 the measured electron density is compared with the results of the model. A good agreement is observed. In the beginning of the arc channel temperature equilibration takes about 60% of the Ohmic input and ionization of argon atoms needs the remaining 40%.

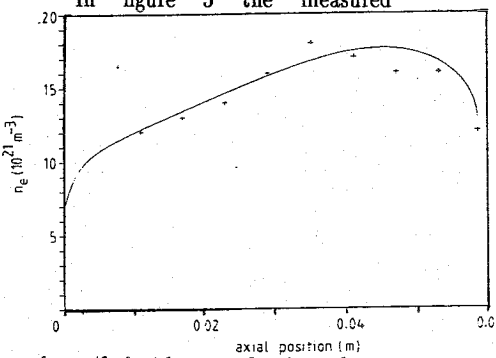

Fig 5: Experimental (crosses) and calculated (line) electron density vs axial position.

The calculated profiles have been obtained by taking the first measured values of the electron density, electron temperature and plasma pressure as starting values, and adjusting the starting value of the gas temperature to give the best fit to the measurements. Once the starting conditions are set, the complete axial profile is determined by Runge–Kutta integration. The experimental results have been obtained in an arc with a diameter D of 4mm. However, in order to give a good fit to the measurements, an effective diameter of 3.8 mm is used for the model calculations.

REFERENCES

[1] KROESEN G.M.W., PH. D. thesis, Univ. of Techn. Eind., the Netherlands (1988)
[2] Bachmann P.K., Beulens J.J., Kroesen G.M.W.,Lydtin H, Schram D.C. and Wiechert D.U., to be published at the TMS conference, aug.28–sept.1 1989.
[3] Savvides N. and Window B., J. Vac. Sci. Technol. A3, 2386, 1985.
[4] Savvides N.,J. Appl. Phys. 59,4133,1986.
[5] Griem H.R.,"Spectral line broadening by plasmas", Academic press, New York, USA(1974).
[6] Sobel'man, "Introduction to the theory of atomic spectra", Pergamon press, Oxford (1972)
[7] Drawin H.W. and Felenbok P., "Data for plasmas in LTE", Gauthier–Villars, Paris(1965).
[8] J.C.M. de Haas, Ph. D. thesis, Univ. of Techn. Eindh., the Netherlands (1986).
[9] C.J. Timmermans, R.J. Rosado and D.C. Scram, Z. Naturforschung 40A(1985)810.
[10] M. Mitchner and C.J. Kruger Jr., "Partially ionized gases", Wiley,. NY USA (1973).
[11] J.A. Owczarek, "Fundamentals of gas dynamics", International Textbook Company, Scranton USA (1964).